

## RAFT-Mediated Emulsion Polymerization of Styrene with Low Reactive Xanthate Agents: Microemulsion-like Behavior

Mark P. F. Pepels,<sup>†</sup> Clovia I. Holdsworth,<sup>‡</sup> Sagrario Pascual,<sup>§</sup> and Michael J. Monteiro<sup>\*\*†</sup>

<sup>†</sup>Australian Institute for Bioengineering, Nanotechnology, The University of Queensland, Brisbane QLD 4072, Australia, <sup>‡</sup>Centre for Organic Electronics, School of Environmental and Life Sciences, University of Newcastle, Callaghan, NSW 2308, Australia, and <sup>§</sup>UCO2M-UMR CNRS6011, LCOM-Chimie des Polymères, Université du Maine, Avenue Olivier Messiaen, 72085 Le Mans Cedex 9, France

Received June 2, 2010; Revised Manuscript Received July 11, 2010

**ABSTRACT:** Xanthates ([1-(*O*-ethylxanthyl)ethyl]benzene (**CTA1**) and [1-(*O*-trifluoroethylxanthyl)ethyl]benzene (**CTA2**) have the capacity to control the molecular weight distribution in emulsion polymerizations to produce very small nanoparticles below 20 nm. We form stable translucent polystyrene latexes using surfactant (sodium dodecyl sulfate, SDS) and a small amount of pentanol as cosurfactant. The high CTA concentration results in a greater retardation in rate until consumption of all the RAFT agent. With an increase in **CTA1** the particle size decreases from 38 to 8 nm and the particle number concentration  $N_c$  increases from  $2 \times 10^{18}$  to  $2 \times 10^{20}$  particles/L. Although an increase in  $N_c$  should in principle lead to a faster rate of polymerization, we observe a greater retardation in rate with increasing CTA. The higher  $C_{lr,RAFT}$  of **CTA2** results in a greater initial retardation until consumption of all the RAFT agent and particle diameters lower than 5 nm and at high concentrations of **CTA2** diameters that are not measurable. Kinetic simulations solving the Smith–Ewart equations explain the anomaly between  $R^*$  (formed from the fragmentation of the R group from the RAFT agent) acting to nucleate micelles and terminate radicals within particles. The small and mobile  $R^*$  radicals can exit particles, re-enter micelles or other particles, re-exit until they either nucleate micelles, or terminate with propagating polymeric chains. This process of exit and re-entry is similar to limit 3 in a conventional emulsion polymerization. The higher micelle nucleation rate through initiation within micelles by  $R^*$  radicals results in smaller and a greater number of particles. Exit is the dominant mechanism for greater nucleation and retardation.

### Introduction

The versatile “living” radical polymerization (LRP) techniques produce polymers with controlled molecular weight distributions (MWDs) and architectures. These techniques comprise (i) reversible addition–fragmentation chain transfer (RAFT),<sup>1</sup> (ii) atom transfer radical polymerization (ATRP),<sup>2</sup> (iii) nitroxide-mediated polymerization (NMP),<sup>3</sup> and (iv) metal-catalyzed radical polymerization (e.g., single electron transfer LRP),<sup>4,5</sup> all of which produce new, interesting, and responsive (smart) polymeric structures and materials. All techniques have the capability to control the polymerization of a vast number of functional monomers, in a wide range of acceptable solvents, and over a wide range of temperatures.

Heterogeneous (or emulsion) polymerizations have become the most attractive industrial method for making a wide variety of polymer products.<sup>6,7</sup> The major advantages for conducting polymerizations in dispersed media over bulk or solution include (i) the use of environmentally friendly medium, usually water, (ii) the use of a broad range of monomers under a wide range of experimental conditions, and (iii) the excellent heat transfer that provides better control of the reaction temperature and thus better control of the final polymer latex size and molecular weight distributions. Polymerizations in confined or compartmentalized particles on the nanoscale result in a significant increase in the rate of polymerization, rapidly reaching high conversions with low monomer residuals. The resultant polymer forms in high

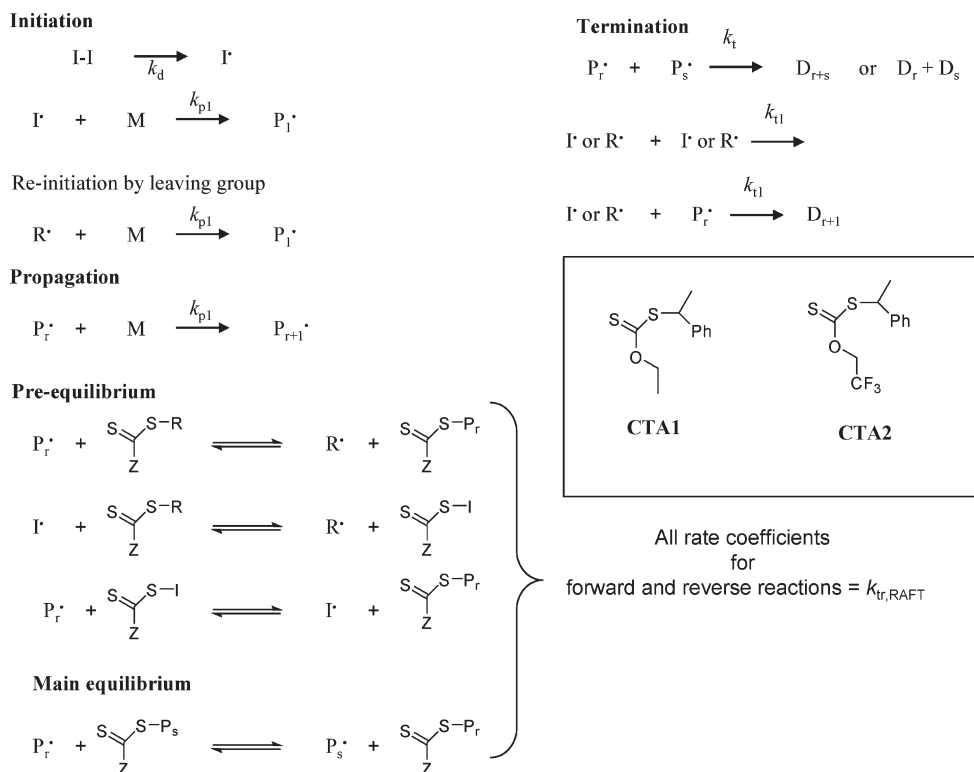
solids (~50 wt %) in a low-viscosity environment, which is easy to process. On the basis of all these significant advantages of heterogeneous polymerization over solution or bulk, it is not surprising that being able to carry out LRP via an emulsion process to create polymers with well-defined molecular weight distributions (MWDs), controlled latex particle size distributions (PSD), and novel particle morphologies will invariably open a new class of polymer materials for use in the coatings industry and as specialty polymers.

Implementation of RAFT in heterogeneous polymerizations is not as easy as originally believed.<sup>8</sup> Previous work involving RAFT *ab initio* emulsion polymerization with a highly reactive chain transfer agent (CTA) reveals problems of retardation and colloidal instability.<sup>8,9</sup> In addition, this system fails to produce well-defined molecular weight distributions and fails to control the particle size distributions (usually broad). The main reason for this failure is due to the slow transportation<sup>10,11</sup> of the highly reactive CTA from the droplets to the growing particles. Problems of transportation are overcome by conducting emulsion polymerizations with multistep processes,<sup>12</sup> using surfactant-like RAFT agents,<sup>13</sup> or conducting the polymerizations in miniemulsions<sup>14</sup> or seeded<sup>10</sup> emulsions. Success of these methods relies on the capture of the RAFT agent inside the growing particles. Recent work by our group shows that a thermoresponsive nanoreactor successfully produces well-defined polymer but, more importantly, produces narrow and predictable PSDs.<sup>15</sup>

Microemulsions present an alternative method to conduct RAFT-mediated polymerizations. They are transparent emulsions with thermodynamic stability and allow the synthesis of

\*To whom correspondence should be addressed. E-mail: m.monteiro@uq.edu.au.

Scheme 1. Kinetic Scheme from the RAFT to the Simplified Degenerative Chain Transfer Process



very small particles with diameters between 10 and 50 nm.<sup>16</sup> The process involves a large amount of surfactant, generally well above its critical micellar concentration (cmc), to stabilize tiny monomer-swollen micelles in a continuous aqueous medium. In many ways, this system is analogous to miniemulsions. Surprisingly, there have been only a few publications on the RAFT-mediated polymerizations in direct<sup>17,18</sup> and inverse<sup>19</sup> microemulsion polymerizations. Recently, Sogabe and McCormick<sup>19</sup> have published the first study on RAFT-mediated inverse microemulsion for the homopolymerization of *N,N*-dimethylacrylamide and the block copolymerization with *N,N*-diethylacrylamide.

The very high surfactant loadings used in microemulsions limits their use in many applications. Pan and co-workers<sup>20,21</sup> significantly decreased the amount of surfactant through a modified microemulsion process they termed “differential microemulsion polymerization”. Their process, for example, relied on the slow feed of a mixture of styrene and a small amount of pentanol into the reaction vessel containing sodium dodecyl sulfate (SDS), water, and ammonium persulfate (APS) to maintain a translucent reaction throughout the polymerization. The particle size ranged between 35 and 25 nm, controlled by the amount of SDS—the greater the SDS, the lower the particle size.

In this work, we used identical conditions to He and Pan<sup>21</sup> but in a one-pot reaction to conduct RAFT-mediated polymerizations of styrene with low reactive xanthates<sup>22</sup> ([1-(*O*-ethylxanthyl)ethyl]benzene (**CTA1**) and [1-(*O*-trifluoroethylxanthyl)ethyl]benzene (**CTA2**)) under *ab initio* emulsion conditions (Scheme 1). The initial opaque reaction mixture contained monomer droplets, but after the loss of monomer droplets in the system, the reaction polymerization mixture became translucent with a slight blue hue. These RAFT agents were chosen because they have (i) the same leaving R group and allowed us to study the effect of exit and its dependence upon the chain transfer constant,  $C_{tr,RAFT}$ , and (ii) have been shown to be well-behaved in all dispersion polymerizations in which the  $M_n$ s and PDIs found in these systems are close to that found in solution or bulk experiments.<sup>23–25</sup> Pentanol has previously been used in combination with SDS to reduce the interfacial

tension to spontaneously form a microemulsion.<sup>26</sup> Therefore, the addition of pentanol in our *ab initio* system allows us to attain a high weight percentage of styrene ( $\alpha = 13.4\%$ ) and low weight percentage of surfactant ( $\gamma = 3.3\%$ ), where  $\alpha = \text{monomer}/(\text{monomer} + \text{water}) \times 100$  and  $\gamma = \text{surfactant}/(\text{surfactant} + \text{monomer} + \text{water}) \times 100$ . We find that both CTAs result in retardation in the rate of polymerization, and the MWDs, in particular the number-average molecular weight,  $M_n$ , and polydispersity index, PDI, were close to theoretical prediction for bulk polymerizations.<sup>5,27</sup> The particle size remains relatively constant over the reaction consistent with findings for most microemulsion polymerizations. In addition, an increase in the RAFT agent concentration leads to a decrease in the particle diameter from 38 nm without CTA down to 8 nm with **CTA1**. This work provides a methodology to prepare small nanoparticles with controlled MWDs because of the high exit rate of the R group from the RAFT agent.

## Experimental Section

**Materials.** All *ab initio* polymerizations use Milli-Q water (18.2  $M\Omega \text{ cm}^{-1}$ ) generated from a Millipore Milli-Q-Academic Water Purification System. Styrene (STY, Sigma-Aldrich, 99%) was passed through a column of basic alumina (standard grade, Sigma-Aldrich). Sodium dodecyl sulfate (SDS, ICN, Ultra pure), ammonium persulfate (APS, AR grade, APS Chemicals, 98%), 1-pentanol (Sigma-Aldrich, 99%), tetrahydrofuran (THF, HPLC grade, LABSCAN, 99.8%), 2,2,2-trifluoroethanol (Sigma-Aldrich, 99%), carbon disulfide ( $\text{CS}_2$ , Sigma-Aldrich, 99.9%), *N,N*-dimethylformamide (DMF, Lab Scan, 99.8%), sodium hydroxide (60% in mineral spirit, Aldrich), (1-bromoethyl)benzene (Aldrich, 97%), magnesium sulfate anhydrous ( $\text{MgSO}_4$ , Amresco), diethyl ether (ACS grade, Merck), petroleum spirit (bp 40–60 °C, AR grade, Ajax, 90%), and ethyl acetate (AR grade) were used as received.

**Synthesis of Chain Transfer Agents.** [1-(*O*-Ethylxanthyl)ethyl]benzene (**CTA1**). **CTA1** was synthesized according to the literature procedure.<sup>28</sup>

[1-(*O*-Trifluoroethylxanthyl)ethyl]benzene (**CTA2**)<sup>29</sup>. To a stirred solution of trifluoroethanol (1.4 mL, 19.5 mmol) in

DMF (14 mL) at 0 °C under argon, a mixture of CS<sub>2</sub> (2.6 mL, 43.1 mmol) and sodium hydroxide in mineral oil (0.967 g, 24.2 mmol) was gradually added over a period of 10 min. Upon complete addition, the reaction mixture was stirred for 45 min at 0 °C. (1-Bromoethyl)benzene (2.5 mL, 17.7 mmol) was added dropwise, and the mixture stirred overnight at 25 °C. The mixture was diluted with 50 mL of diethyl ether and washed 3 times with Milli-Q water and 3 times with brine. The organic phase was then dried over anhydrous magnesium sulfate and filtered, and the solvents were removed under vacuum. Purification by column chromatography (first petroleum spirit, second 95:5 petroleum spirit/ethyl acetate) gave the desired product. After drying under vacuum 4.22 g of product was obtained (85% yield). <sup>1</sup>H NMR (CDCl<sub>3</sub>, 300 MHz): δ = 1.75 (3H, d, CH<sub>3</sub>-CH(Ph)-S), 4.88 (3H, m, F<sub>3</sub>C-CH<sub>2</sub>-O and S-CH(Ph)-CH<sub>3</sub>), 7.30 (5H, m, aromatic protons). Element analysis calcd (%) for C<sub>11</sub>H<sub>11</sub>F<sub>3</sub>OS<sub>2</sub>: C 47.13%, H 3.96%, S 22.88%. Found: C 47.17%, H 4.2%, S 23.54%.

**Techniques.** *Size Exclusion Chromatography (SEC).* All polymer samples were dried in a vacuum oven for 2 days at 25 °C, dissolved in THF to a concentration of 1 mg/mL, and then filtered over a 0.45 μm PTFE syringe filter. Analysis of the molecular weight distributions of the polymers was accomplished by using a Waters 2695 separations module, fitted with a Waters 410 refractive index detector held at a constant temperature of 35 °C, a Waters 996 photodiode array detector, two Ultrastaygel linear columns (7.8 × 300 mm), and one Styragel linear column kept in series. These columns were held at a constant temperature of 40 °C for all analyses. The columns used separate polymers in the molecular weight range of 500–6 × 10<sup>6</sup> g/mol with high resolution. THF was the eluent used at a flow rate of 1.0 mL/min. Calibration was carried out using narrow molecular weight PSTY standards (PDI ≤ 1.1) ranging from 500 to 2 × 10<sup>6</sup> g/mol. Data acquisition was performed using Empower software, and molecular weights were calculated relative to polystyrene standards.

<sup>1</sup>H Nuclear Magnetic Resonance (NMR). All NMR spectra were recorded on a Bruker DRX 500 MHz spectrometer using an external lock (D<sub>2</sub>O, CDCl<sub>3</sub>).

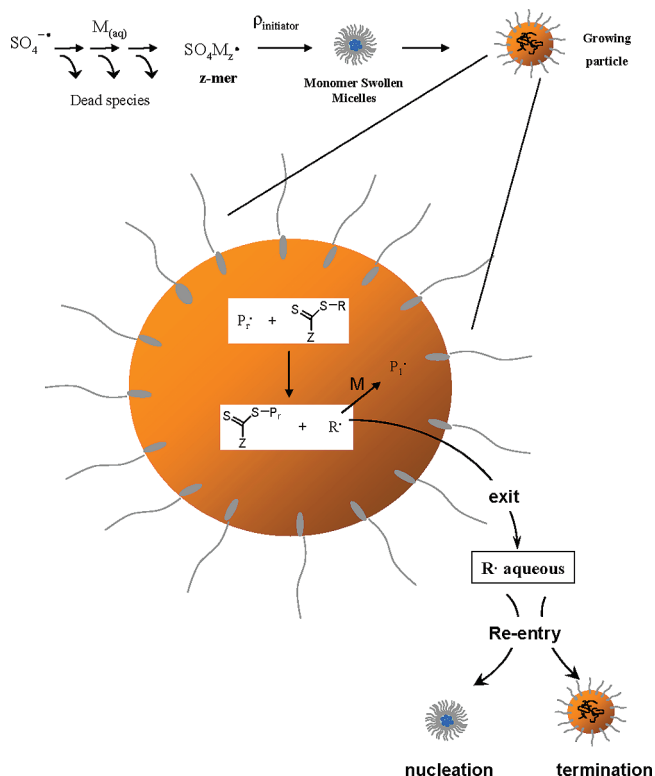
*Dynamic Light Scattering (DLS).* Dynamic light scattering measurements were performed using a Malvern Zetasizer 3000HS. The sample refractive index (RI) was set at 1.59 for polystyrene. The dispersant viscosity was set to 0.89 N·s/m<sup>2</sup>. The number-average particle diameter, Z-average, and particle PDI were measured for each sample.

*Ab Initio RAFT-Mediated Polymerization of Styrene.* A typical *ab initio* RAFT-mediated polymerization of styrene was as follows. A mixture of styrene (3.5 mL, 3.5 × 10<sup>-2</sup> mol), CTA1 (86.43 mg, 3.82 × 10<sup>-4</sup> mol), and 1-pentanol (50 μL) was added to a 50 mL round-bottom Schlenk flask containing Milli-Q water (21 mL) and SDS (0.827 g, 2.9 × 10<sup>-3</sup> mol). APS (0.0174 g, 7.64 × 10<sup>-5</sup> mol) was added, and the mixture was purged with argon for 20 min. For this polymerization weight percentages are α = (oil/(oil + water)) × 100 = 13.2% and γ = (surfactant/(surfactant + oil + water)) × 100 = 3.3%. To start the polymerization, the mixture was heated to 70 °C (t = 0) and kept under a positive argon pressure during the reaction. Samples were taken periodically with a syringe to monitor conversion (gravimetry), particle size (DLS), and molecular weight distribution (SEC). In experiments where CTA is added, the reaction mixture during polymerization turns from opaque to translucent once monomer droplets have been consumed.

## Theoretical Discussion

**Kinetic Modeling of RAFT-Mediated Dispersion Polymerization.** The kinetic simulations solve the Smith–Ewart equations<sup>30</sup> for RAFT-mediated dispersion polymerizations. The specific purpose of these simulations is to examine the effect of exit through reactions with CTA on the rate of

**Scheme 2. Main Kinetic Events for RAFT-Mediated *ab Initio* Polymerization, Including Entry and Exit of R\***



polymerization. We are not trying to simulate an *ab initio* polymerization with its complex nucleation and partitioning processes but use the simulations to examine the effect of exit of the R leaving group from the RAFT agent on the rate of polymerization. In this work, we use two RAFT agents that show little or no retardation in solution or bulk experiments with styrene,<sup>22,31</sup> and therefore we can simplify the RAFT mechanism from including all the intermediate radicals to degenerative chain transfer (Scheme 1). This is an accurate method to simulate RAFT-mediated polymerizations in solution or bulk providing that retardation in rate is not observed.<sup>32,33</sup> Our model does not account for the complex nucleation process but assumes that the initial micelle size is close to that of the final particle size. This assumption is valid after about 5% conversion as the particle size remains relatively constant to full conversion in our styrene emulsion experiments (see data in the Results and Discussion section). This is also valid for microemulsion polymerizations.<sup>34</sup>

Scheme 2 gives the main kinetic events for a RAFT-mediated emulsion where the system is compartmentalized, and there are no monomer droplets present. First, a thermal initiator decomposes in the aqueous phase to form radicals, I\*, that then adds to monomer. These radicals continue to add to monomer and on their way to becoming surface-active radicals survive termination events with all other radicals in the aqueous phase ([I\*]<sub>aq</sub>). When they reach a critical length (of z monomer units or a “z-mer”), they become surface active and enter a particle or micelle. The pseudo entry rate coefficient, ρ<sub>initiator</sub>, for radicals derived from initiator is given by the following equation<sup>6,35</sup>

$$\rho_{\text{initiator}} = \frac{2k_d[I]N_A}{N_c} f_{\text{efficiency}} \quad (1)$$

where  $k_d$  is the rate coefficient for initiator decomposition, [I] is initiator concentration,  $N_A$  is Avogadro's number,  $N_c$  is

**Table 1. Parameters Used in the Kinetic Simulations for the RAFT-Mediated Microemulsion Polymerization of Styrene at 70 °C**

parameter	value	description	literature reference
$C_p$	3 mol L <sup>-1</sup>	monomer concentration within the particle	18, 41
$D_p$	20 nm	diameter of the particle	
$N_c$	1 × 10 <sup>20</sup> particles L <sup>-1</sup>	number of particles per L	
$k_p$	477 L mol <sup>-1</sup> s <sup>-1</sup>	propagation rate coefficient	45
$k_{p1}$	4770 L mol <sup>-1</sup> s <sup>-1</sup>	propagation rate coefficient for R* + M	
$k_t, k_{t1}$	1.72 × 10 <sup>8</sup> L mol <sup>-1</sup> s <sup>-1</sup>	termination rate coefficient	33
$k_d$	2.2 × 10 <sup>-6</sup> s <sup>-1</sup>	initiator decomposition rate coefficient	46
$D_R$	1 × 10 <sup>-7</sup> dm <sup>2</sup> s <sup>-1</sup>	diffusion coefficient of R*	47
$q$	1279	partition coefficient of R*	38

the number of particles per liter, and  $f_{\text{efficiency}}$  is the efficiency to form a  $z$ -mer radical from initiator-derived radicals, I\*.

In styrene emulsions where the size of the micelles and particles are small, instantaneous termination occurs when a  $z$ -mer enters a particle already containing a growing radical. This “zero–one” condition permits only one or zero radicals to reside in a particle at any one time. In conventional emulsions, the “zero–one” condition occurs when the probability of termination of a  $z$ -mer is high compared to propagation. To satisfy this requirement, the rate coefficient for propagation,  $k_p$ , should be low (e.g., for styrene) and the particle size be small. For reactive monomers with a high  $k_p$  (e.g., butyl acrylate) there is a high probability that one or more radicals can coexist per particle even in very small particles.<sup>36</sup> In systems with high surfactant concentrations (i.e., with high number of micelles) as in microemulsions, they are considered for most monomer systems as zero–one since there are ~1000 more micelles than particles, and the probability of a  $z$ -mer entering a particle containing a radical is negligible. However, in many systems termination by a  $z$ -mer may be non-negligible.<sup>37</sup>

Small radicals formed within the particles through chain transfer to monomer or CTA have a high probability of exiting the small micelles or particles.<sup>8,25,38,39</sup> The rate coefficient for exit depends on the diffusion coefficient ( $D_R$ ) of the radical, its partition coefficient ( $q$ ) between the oil and water phases, and the radius of the swollen particle ( $r_s$ ) and is given as follows:<sup>40</sup>

$$k_{\text{exit}} = \frac{3D_R}{qr_s} \quad (2)$$

These exited R\* radicals can either terminate in the aqueous phase or re-enter a micelle or particle with rate coefficient:

$$k_{\text{re-entry}} = 4\pi D_R N_A r_s \quad (3)$$

and therefore

$$\rho_{\text{re-entry}} = k_{\text{re-entry}} [\text{R}^*]_{\text{aq}} \quad (4)$$

The re-entry of R\* into a micelle of ~3 nm would occur quite rapidly due to the great number of micelles but would also rapidly re-escape due to their very small size (limit 3 in emulsion polymerization<sup>6</sup>). This situation will change if they enter the larger polymer particles (~20–40 nm) as exit decreases by an order of magnitude (cf. eq 2). The R\* radicals have a much higher probability to propagate due to the higher monomer concentration in the particles compared to micelles (cf. the Morton equation<sup>41</sup>) or undergo termination if the particles contain a polymeric or other radical species. Therefore, exited radicals play an important role in emulsion systems where the size of the particles are small and have found to retard the rate of polymerization in seeded and *ab initio* emulsion polymerizations with similar RAFT agents used in this work.<sup>23,25,38</sup>

Similar to the derivation by Butte et al.<sup>42</sup> for the Smith–Ewart equations in two dimensions for NMP<sup>43</sup> and Luo et al.<sup>44</sup> for RAFT (but where  $j$  represents the intermediate radical

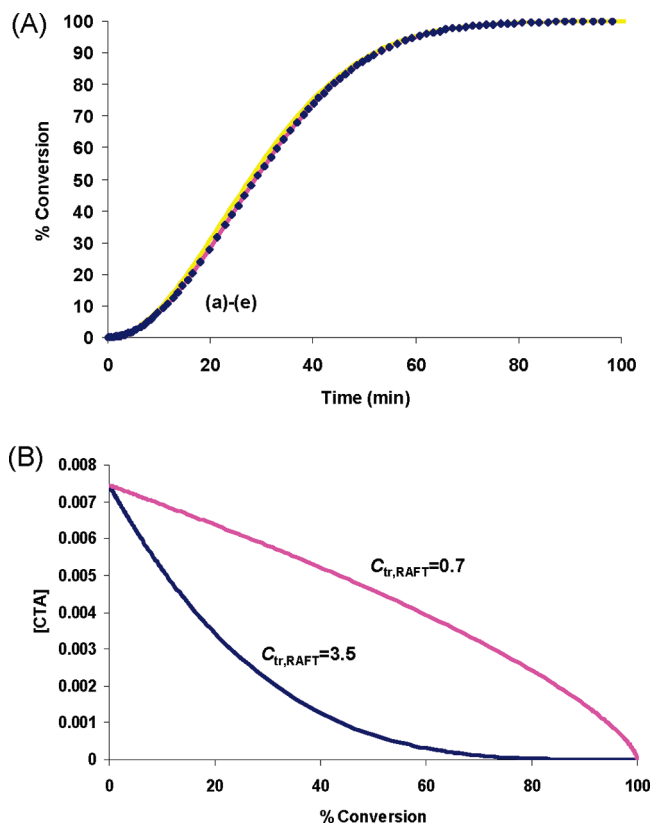


**Figure 1.** (A) Kinetic simulations using parameters in Table 1 with “no exit” using  $[I] = 3.12 \times 10^{-3}$  mol L<sup>-1</sup>. Curves (a) to (e) represent 0, 1, 5, 10, and 20 [CTA]:[I], respectively. (B) Loss of CTA with conversion according to theory.<sup>27,48</sup>

concentration in their derivation of the Smith–Ewart equation), we derive an equation for RAFT. The equation used to describe the number fraction of particles  $N_i^j$ , in which there are  $i$  active polymeric radicals P\* and  $j$  active R\* radicals, is given as follows:

$$\begin{aligned} \frac{dN_i^j}{dt} = & \rho_{\text{initiator}} \{ (1 - \delta_i) N_{i-1}^j - N_i^j \} + k_{\text{exit}} \{ (j+1) N_i^{j+1} \\ & - j N_i^j \} + k_{\text{tr,RAFT}} [\text{CTA}] \{ (1 - \delta_j) (i+1) N_{i+1}^{j-1} - i N_i^j \} \\ & + \frac{k_t}{N_A v_p} \{ (i+1)(i+2) N_{i+2}^j - i(i-1) N_i^j \} \\ & + \frac{k_{t1}}{N_A v_p} \{ (i+1)(i+2) N_{i+1}^{j+1} - ij N_i^j \} + \frac{k_{t1}}{N_A v_p} \\ & \{ (j+1)(j+2) N_i^{j+2} - j(j-1) N_i^j \} + k_{p1} C_p \{ (1 - \delta_i) \\ & (j+1) N_{i-1}^{j+1} - j N_i^j \} + \rho_{\text{re-entry}} \{ (1 - \delta_j) N_i^{j-1} - N_i^j \} \\ & + k_{\text{tr,RAFT}} [\text{MacroCTA}] \{ (1 - \delta_i) (j+1) N_{i-1}^{j+1} - j N_i^j \} \quad (5) \end{aligned}$$

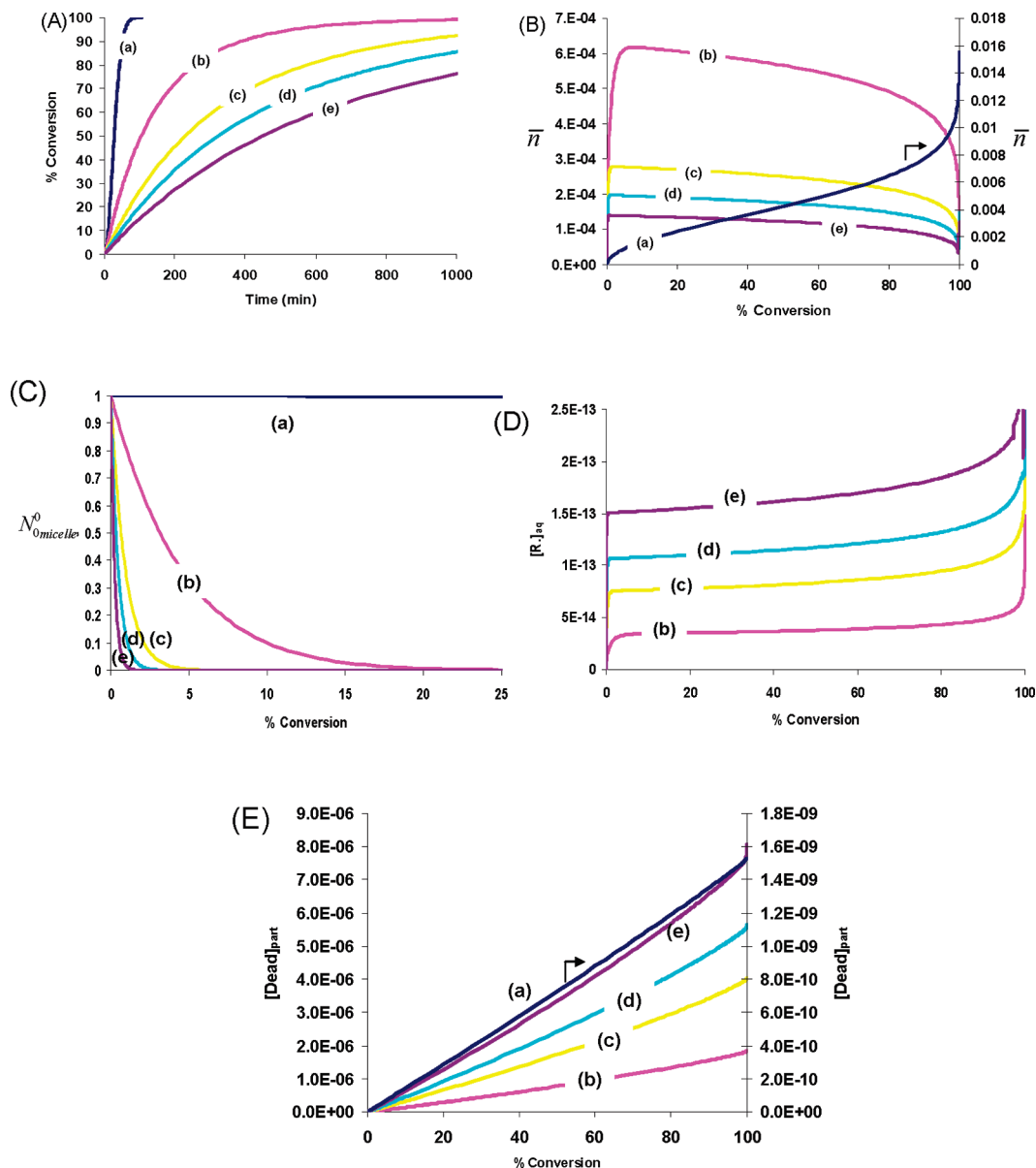


**Figure 2.** Kinetic simulations using parameters in Table 1 with “exit” using  $[I] = 3.12 \times 10^{-3} \text{ mol L}^{-1}$ , in which curves (a) to (e) represent 0, 1, 5, 10, and 20  $[CTA]:[I]$ , respectively.  $C_{tr,RAFT} = 0.7$ . (A) conversion vs time; (B) number of radicals per particles ( $\bar{n}$ ) vs conversion; (C) number fraction of particles converted to particles by z-mers or exited  $R^*$  radicals vs conversion; (D)  $[R^*]_{aq}$  vs conversion and (E) [dead polymer] within the particles vs conversion. Curve a in (B, E) have their axis on the right-hand side.

where  $k_{tr,RAFT}$  is the transfer rate coefficient to the RAFT agent (CTA),  $v_p$  is the volume of a swollen particle,  $C_p$  is the monomer concentration within the particles,  $k_t$  is the termination rate coefficient between two polymeric chains,  $k_{t1}$  is the termination rate coefficient dominated by short chains, and MacroCTA consists of a polymer chain with a RAFT end-group. The Kronecker delta  $\delta_i$  or  $\delta_j$  in eq 5 represents the condition if  $i$  or  $j$  equals 0, then the Kronecker delta value equals 1. We set that the initial particle number to remain constant but include in the model the number fraction of particles that are converted to particles by z-mers or exited  $R^*$  radicals,  $N_0^0$ , and those not yet stung or still existing as micelles,  $N_{0,micelles}^0$ . The initial conditions are  $N_{0,micelles}^0 = 1$  and  $N_0^0 = 0$ , and therefore additional terms (eqs 6–8) must be included in the full differential equation in eq 5 for  $N_0^1$ .

$$\frac{dN_0^1}{dt} = \rho_{initiator} N_{0,micelles}^0 \quad (6)$$

$$\frac{dN_0^1}{dt} = \rho_{re-entry} N_{0,micelles}^0 \quad (7)$$

and

$$\frac{dN_{0,micelles}^0}{dt} = -(\rho_{initiator} + \rho_{re-entry}) N_{0,micelles}^0 \quad (8)$$

The average number of  $P^*$  ( $\bar{n}$ ) per particle is given by

$$\bar{n} = \sum_i \sum_j i N_i^j \quad (9)$$

The differential equations for all other species are given as follows:

$$\frac{dC_p}{dt} = -k_{p1} C_p [R^*] - k_p C_p [P^*] \quad (10)$$

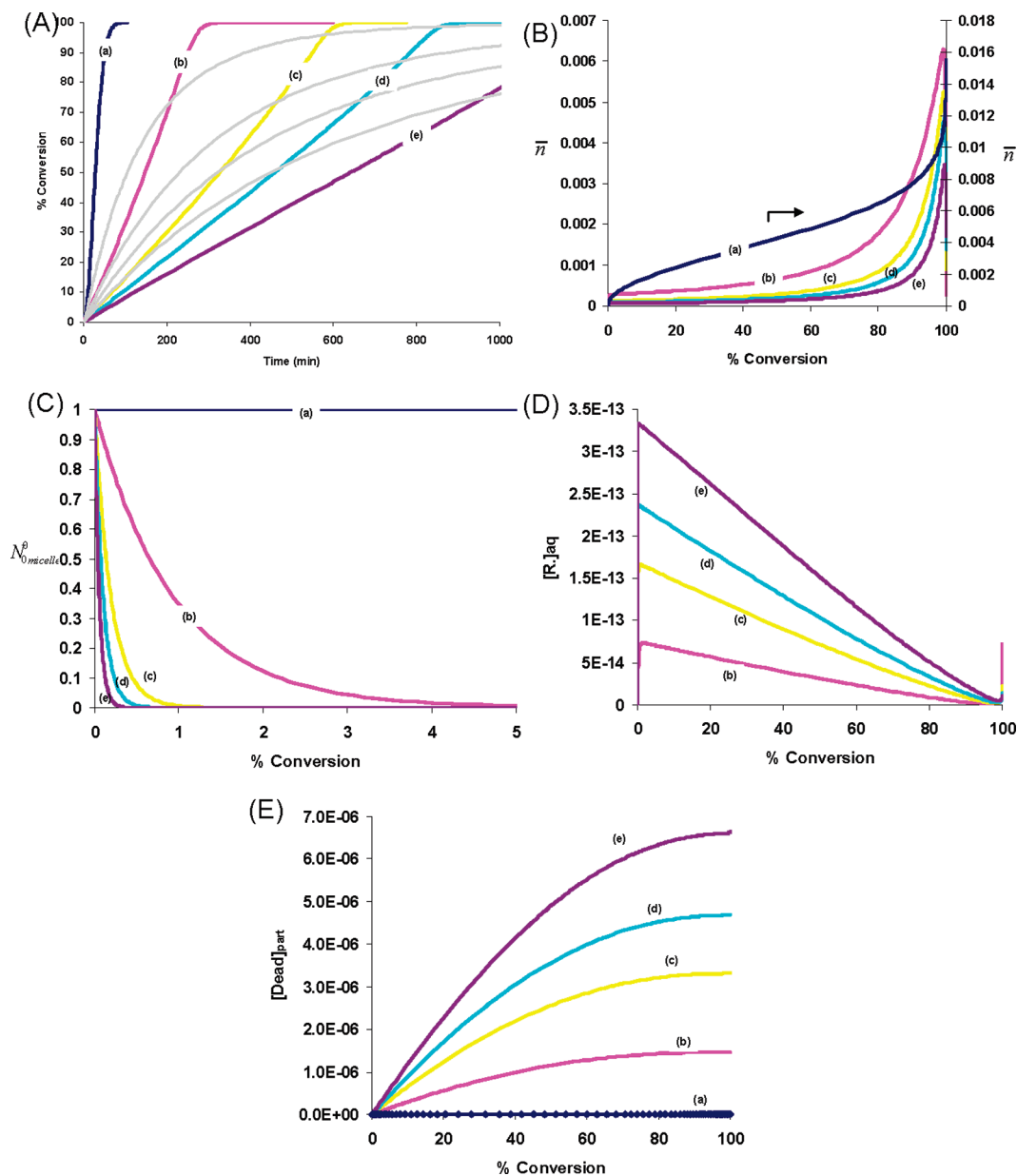


**Figure 3.** Kinetic simulations using parameters in Table 1 with “exit” using  $[I] = 3.12 \times 10^{-3} \text{ mol L}^{-1}$ , in which curves (a) to (e) represent 0, 1, 5, 10, and 20  $[CTA]:[I]$ , respectively.  $C_{tr,RAFT} = 3.5$ . (A) Conversion vs time; (B) number of radicals per particles ( $\bar{n}$ ) vs conversion; (C) number fraction of particles converted to particles by  $z$ -mers or exited  $R^*$  radicals vs conversion; (D)  $[R^*]_{aq}$  vs conversion and (E)  $[dead\ polymer]$  within the particles vs conversion.

$$\frac{d[I]}{dt} = -k_d[I] \quad (11)$$

$$\frac{d[CTA]}{dt} = -k_{tr,RAFT}[CTA][P^*] + k_{tr,RAFT}[MacroCTA][R^*] \quad (12)$$

$$\frac{d[R^*]_{aq}}{dt} = k_{exit}[R^*]N_c/N_A - k_{entry}[R^*]_{aq}N_c/N_A - k_{rl}[R^*]_{aq}[T^*]_{aq} \quad (13)$$

The differential equations (5)–(13) are solved iteratively using a high-order Runge–Kutta method.<sup>5,27</sup> Consistency checks are made to ensure that the total number of particles and micelles remained constant with time. We use eq 14 below to calculate  $[T^*]_{aq}$ .

**Kinetic Simulations with “No Exit”.** The first set of kinetic simulations examines the effect of “no exit” by setting  $k_{exit}$  to zero and varying the concentration of **CTA1** (i.e., a CTA with  $C_{tr,RAFT} = 0.7$ ; a value typical for this type of xanthate<sup>22</sup>). The model uses the same concentration of CTA in all particles and neglects partitioning between particles. Table 1 gives all other parameters. Simulations without CTA (Figure 1A, curve a) result in nearly identical conversion–time profiles to those for all **CTA1** concentrations (Figure 1A, curves b–e). Simulations with a more reactive CTA (i.e., **CTA2** with a  $C_{tr,RAFT} = 3.5$ <sup>22</sup>) also show near-identical profiles to that without CTA regardless of the concentration of **CTA2** (data not given). Without exit these simulations result in negligible retardation in rate.

The theoretical consumption of CTA in solution or bulk<sup>27</sup> over conversion is slightly different between the two CTAs (Figure 1B). Consumption of **CTA2** is faster than **CTA1**, with full consumption after 70% conversion. Extending this

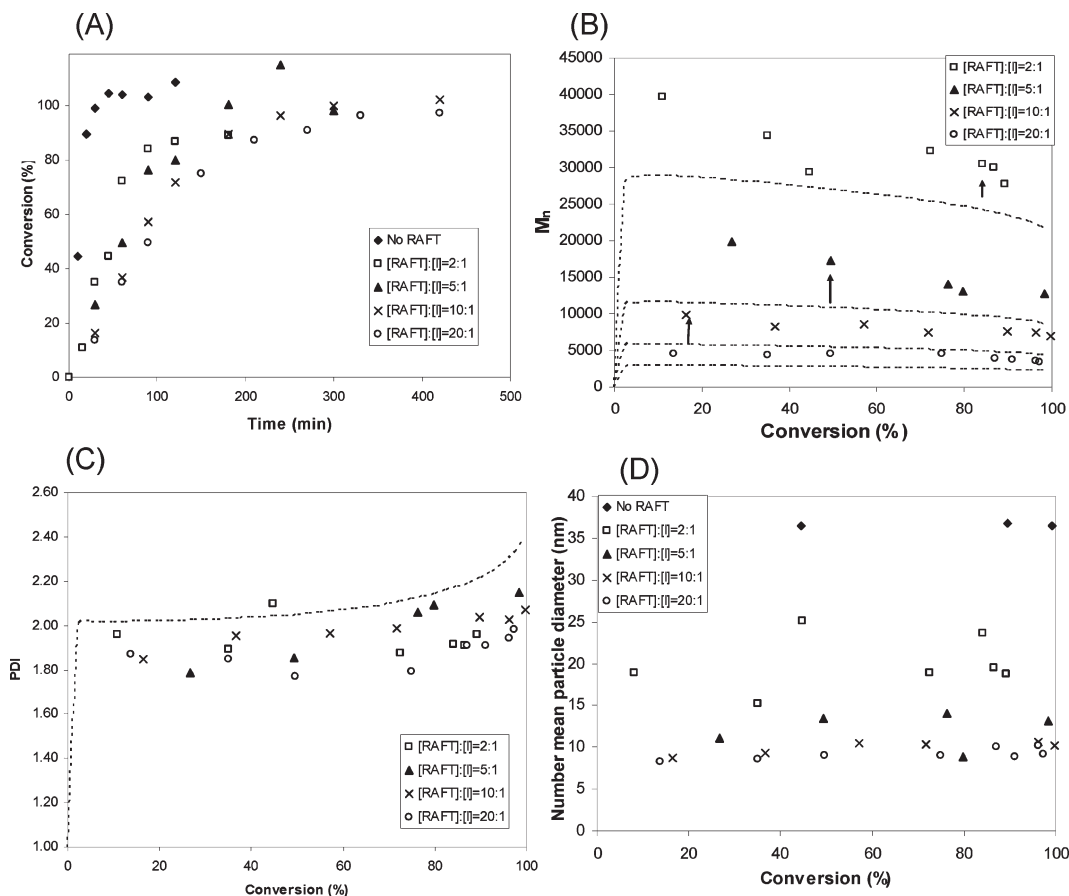


**Figure 4.** Kinetic data for the RAFT-mediated emulsion polymerization of styrene at 70 °C varying **CTAI** ([1-(*O*-ethylxanthyl)ethyl]benzene). (A) conversion vs time, (B) number-average molecular weight ( $M_n$ ) vs conversion, (C) polydispersity index (PDI) vs conversion, and (D) particle diameter vs conversion.  $[I] = 3.12 \times 10^{-3} \text{ mol L}^{-1}$ . Dashed lines are from theory.<sup>49</sup>

into *ab initio* suggests there will be high CTA concentration levels even at conversions as high as 50%. Should the CTA influence the rate, we would expect this influence to be effective over much of the conversion range.

**Kinetic Simulations with “Exit”.** Simulations of **CTAI** with  $C_{ir,RAFT} = 0.7$ . The second set of simulations examines the effect of exit by varying the concentration of **CTAI** and by assuming that the partition coefficient of  $R^*$  radicals is identical to styrene due to their similarity in chemical structure. These simulations generate conversion–time profiles with a significant retardation in rate with increasing **CTAI** concentration (Figure 2A). The simulations also show that the average number of radicals per particles ( $\bar{n}$ ) decrease with increasing **CTAI** (Figure 2B), suggesting that these exited  $R^*$  radicals act to reduce the number of active growing radicals within the particles. In addition, the extremely low values of  $\bar{n}$  (i.e., well below 0.5) should result in particles that obey the zero–one condition for styrene.

The small size of both particles and micelles allows rapid exit (or escape) of  $R^*$  radicals due their high exit rate coefficient, resulting in these radicals being able to explore significantly more micelles and particle than for emulsions in the absence of CTA. In the absence of CTA, *z*-mers enter only a small fraction of micelles (Figure 2C). Even at the lowest **CTAI** concentration, exited radicals enter all the micelles at a conversion less than 20%, and this conversion decreases with increasing CTA. However, although this does not necessarily mean nucleation of micelles to form a growing particle, there is a high probability for greater nucleation. This mechanism will also result in an increase in the water phase of both the radical concentration and the rate of

termination. The aqueous phase concentration of  $R^*$  ( $[R^*]_{aq}$ ) increases from  $1 \times 10^{-14} \text{ M}$  (at 20% conversion) at the lowest **CTAI** concentration to  $1.5 \times 10^{-13} \text{ M}$  (at 20% conversion) at the highest **CTAI** concentration (Figure 2D). These concentrations, however, are still orders of magnitude lower than aqueous phase radical produced from initiator ( $[T^*]_{aq} \sim 8 \times 10^{-9} \text{ M}$ ). Applying the steady-state assumption,  $[T^*]_{aq}$  is calculated as follows:

$$[T^*]_{aq} = \left( \frac{k_d[I]}{k_{t1}} \right)^{0.5} \quad (14)$$

Such a substantially lower  $[R^*]_{aq}$  compared to  $[T^*]_{aq}$  and the decrease of  $\bar{n}$  points toward termination within the particles as the cause of retardation and not a decrease in the pseudo entry rate coefficient due to termination in the aqueous phase. The concentration of dead polymer within the particles in the absence of CTA (Figure 2E, curve a) is very low ( $1.5 \times 10^{-9} \text{ M}$ ) and much lower than the cumulative concentration of initiator-derived radicals ( $\sim 3 \times 10^{-6} \text{ M}$ ) after 75 min. The reason for such a low amount of termination results from the significantly higher probability of *z*-mers to enter and nucleate micelles rather than enter and terminate a growing particle, in agreement with classic microemulsion polymerizations.<sup>49</sup> The addition of **CTAI** in the simulations gives comparable concentrations of dead polymer (curves b–e) to that from initiator-derived radicals. Increasing the **CTAI** concentration results in a higher concentration of exited  $R^*$  that preferentially acts to terminate polymerization.

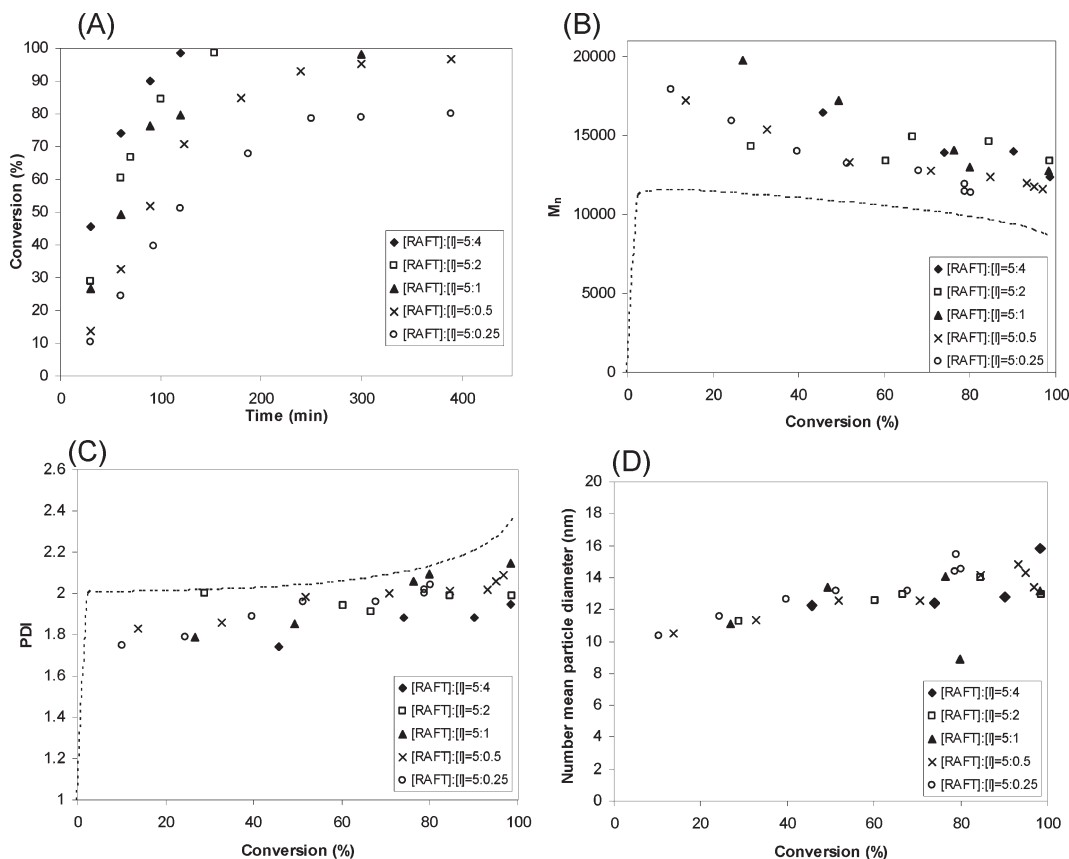


**Figure 5.** Kinetic data for the RAFT-mediated emulsion polymerization of styrene at 70 °C varying initiator concentration in the presence of a constant **CTA1** ([1-(*O*-ethylxanthyl)ethyl]benzene) concentration. (A) conversion vs time, (B) number-average molecular weight ( $M_n$ ) vs conversion, (C) polydispersity index (PDI) vs conversion, and (D) particle diameter vs conversion.  $[\text{CTA1}] = 1.56 \times 10^{-2} \text{ mol L}^{-1}$ . Dashed lines are from theory.<sup>49</sup>

*Simulations of CTA2 with  $C_{\text{tr,RAFT}} = 3.5$ .* In the final set of simulations, we examine the effects of exit using the more reactive **CTA2**. A comparison between the conversion–time profiles for the two CTAs (Figures 2A and 3A) shows at the early stages of polymerization the more reactive **CTA2** generates greater retardation until a conversion of  $\sim 70\%$ , which is the crossover point with **CTA1**. This crossover conversion represents the full consumption of **CTA2** through formation to its MacroCTA (see Figure 1B), after which conversion we observe no retardation but acceleration in rate. The effect of  $\bar{n}$  with increasing  $[\text{CTA}]/[\text{I}]$  ratio (Figure 3B) clearly shows a very different trend to the less reactive CTA, with a slight increase in  $\bar{n}$  with conversion followed by near-exponential increase after 70% conversion. A higher  $C_{\text{tr,RAFT}}$  value results in an initially greater concentration of  $R^*$  in the aqueous phase through exit (Figure 3D) and consequently a much greater entry and nucleation of micelles (Figure 3C). This high frequency of re-entry results in greater concentrations of dead polymer, which rapidly increase to  $\sim 70\%$  monomer conversion and then plateau (Figure 3E).

The simulations show that exit and termination through re-entry into a growing particle causes retardation in the rate of polymerization. These findings are in agreement with simulations in seeded RAFT-mediated emulsions polymerizations.<sup>50</sup> A higher  $C_{\text{tr,RAFT}}$  value results in a greater initial retardation until consumption of all CTA after which time we observe an acceleration in rate. Through this process of exit and re-entry until termination with a growing particle,  $R^*$  can be considered as a relatively “long-lived” radical compared to its lifetime in either solution or bulk. Our simulations clearly show that one does not need to invoke the slow fragmentation<sup>51</sup> or

intermediate termination<sup>52</sup> models<sup>53</sup> to account for retardation in a dispersion (heterogeneous) system.

## Results and Discussion

Even though our RAFT-mediated polymerizations are *ab initio* emulsion polymerizations, the system resembles that of microemulsion polymerizations but in our case with a significantly much lower surfactant concentration. The reasons for this statement are as follows. There is a small and constant particle size over the full conversion range, similar to microemulsion polymerizations. The polymerization mixture turns translucent once monomer droplets have been consumed. The monomer droplets, like the unstung monomer swollen micelles in a microemulsion, will provide a source of monomer to growing particles. Therefore, the kinetic simulations described above should provide insight into the kinetic processes in our *ab initio* system. The  $C_{\text{tr,RAFT}}$  values for **CTA1** and **CTA2** were previously determined in solution experiments to be 0.7 and 3.5, respectively.<sup>22</sup>

**Emulsions Using CTA1 ( $C_{\text{tr,RAFT}} = 0.7$ ).** The first series of *ab initio* emulsion polymerizations of styrene examines the effect of **CTA1** concentration on the rate of polymerizations, molecular weight distribution, and particle size distribution. The emulsion in the absence of **CTA1** showed that the rate of polymerization was fast, reaching full conversion after only 30 min (Figure 4A, curve a). Increasing the concentration of **CTA1** results in a greater decrease in rate (Figure 4A), which is in agreement with the trend found from simulations above. The number-average molecular weight ( $M_n$ ) decreases with increasing concentration of **CTA1** and is close to theoretical values<sup>49</sup> calculated from bulk (Figure 4B). We observe similar agreement between theory and experiment in *ab initio*

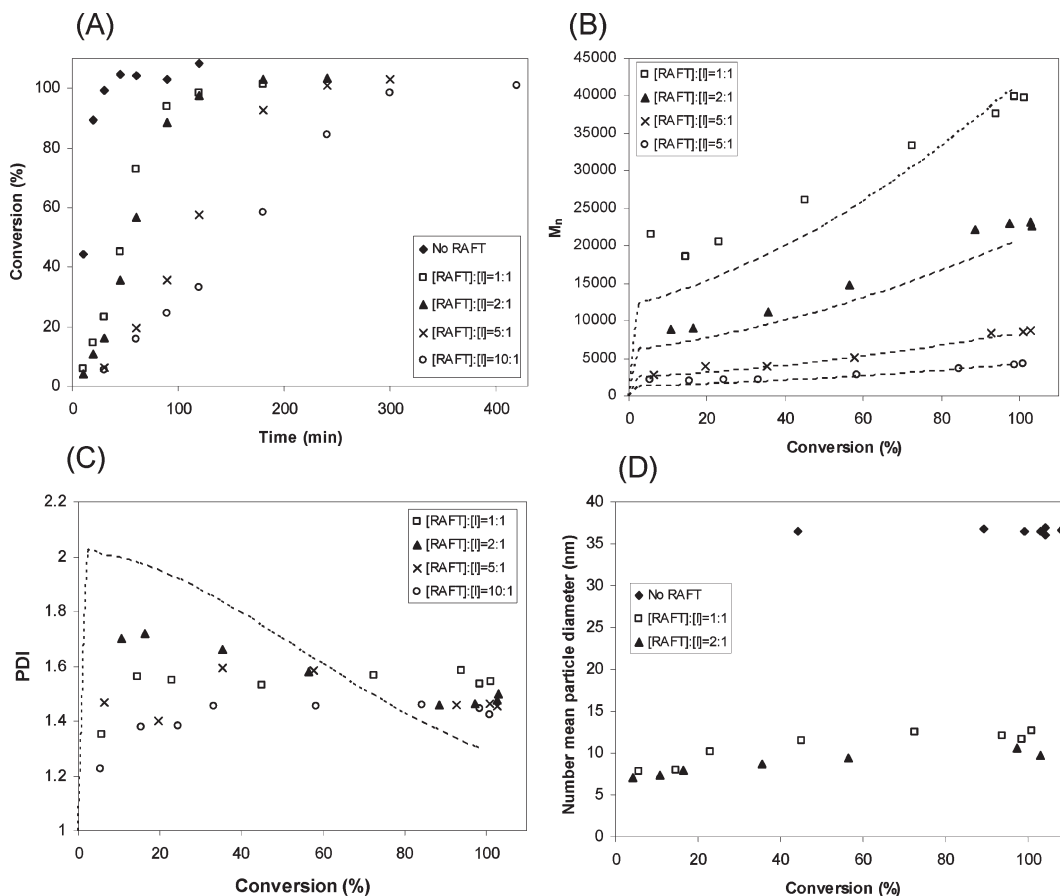


**Figure 6.** Kinetic data for the RAFT-mediated emulsion polymerization of styrene at 70 °C varying **CTA2** ([1-(*O*-trifluoroethylxanthyl)ethyl]benzene). (A) conversion vs time, (B) number-average molecular weight ( $M_n$ ) vs conversion, (C) polydispersity index (PDI) vs conversion, and (D) particle diameter vs conversion.  $[I] = 3.12 \times 10^{-3} \text{ mol L}^{-1}$ . Dashed lines are from theory.<sup>49</sup>

styrene emulsion polymerizations using **CTA1** (see Supporting Information for SEC chromatograms).<sup>23</sup> The results suggest a similar rate of **CTA1** consumption to that of monomer in line with theory (Figure 1B). It also suggests that **CTA1** can partition effectively from non-nucleated micelles or droplets to growing particles. The polydispersity index (PDI) is close to 2 and remains relatively constant over conversion in agreement with theory (Figure 4C).<sup>27</sup> This implies that although the MWD is similar to a bulk polymerization the rate in our microemulsion-like system is substantially more rapid. The reason for this rapid rate is due to compartmentalization of growing radicals within the small nanoreactors.<sup>54</sup> The effect of increasing **CTA1** produces polymer latex particles with a decreasing particle size (Figure 4D), decreasing from 38 nm without CTA to 8 nm at the highest **CTA1**. The particle size remains relatively constant over the conversion range regardless of the concentration of **CTA1**. The number concentration of particles,  $N_c$ , increase from  $2 \times 10^{18}$  particles/L in the absence of CTA to  $2 \times 10^{20}$  particles/L in the presence of 20:1 ([RAFT]:[I]). This result lends support to the high nucleation rate of  $R^*$  through exit and re-entry.

The next set of emulsion polymerizations examines the effect of initiator concentration at a constant concentration of **CTA1**. The rate of polymerization increases with increasing initiator concentration (Figure 5A). There is no effect of initiator concentration on either the  $M_n$  (Figure 5B) or the PDI (Figure 5C) (see Supporting Information for SEC chromatograms). More surprising is that the particle size and particle size evolution with conversion is nearly identical irrespective of the initiator concentration (Figure 5D). These results provide some insight into the dominant mechanistic

role of the  $R^*$  radicals. The rate increase with initiator concentration is commensurate with the increase in the pseudo entry rate coefficient,  $\rho_{\text{initiator}}$  (see eq 1). On the basis of the near-identical particle sizes with increasing initiator concentration, the exited radical  $R^*$  controls and dominates the nucleation process. In addition, these  $R^*$  radicals act as terminators to retard the rate of polymerization. Even with a 4 times increase in initiator concentration, the rate of polymerization is still very much slower than without CTA. Simulation (not shown) with a 4 times initiator concentration at the same CTA concentration shows identical nucleation rates of micelles. The invariance of the MWD on initiator concentration also shows an independence of initiator concentration on termination, most probably due to the very low amount of initiator that has decomposed during the reaction.

**Emulsion Polymerizations using CTA2 ( $C_{\text{tr,RAFT}} = 3.5$ ).** We next examine the effect of the more reactive **CTA2** on the emulsion polymerizations of styrene. The series of polymerizations in Figure 6A show that with an increase in **CTA2** concentration there is a decrease in the rate of polymerization. Comparison between **CTA1** and **CTA2** rates show that **CTA2** generates a greater initial retardation followed by rate acceleration. This is similar to the findings from simulations (Figure 3A). The  $M_n$  decreases with increasing **CTA2** and is close to theory (Figure 6B). The PDI (Figure 6C) is similar for all **CTA2** concentrations remaining relatively constant over conversion and is not as close to theory<sup>27</sup> as that observed for **CTA1** (see Supporting Information for SEC chromatograms). The effect of **CTA2** concentration on the particle size is dramatic (Figure 6D). Even at low concentrations of **CTA2**,

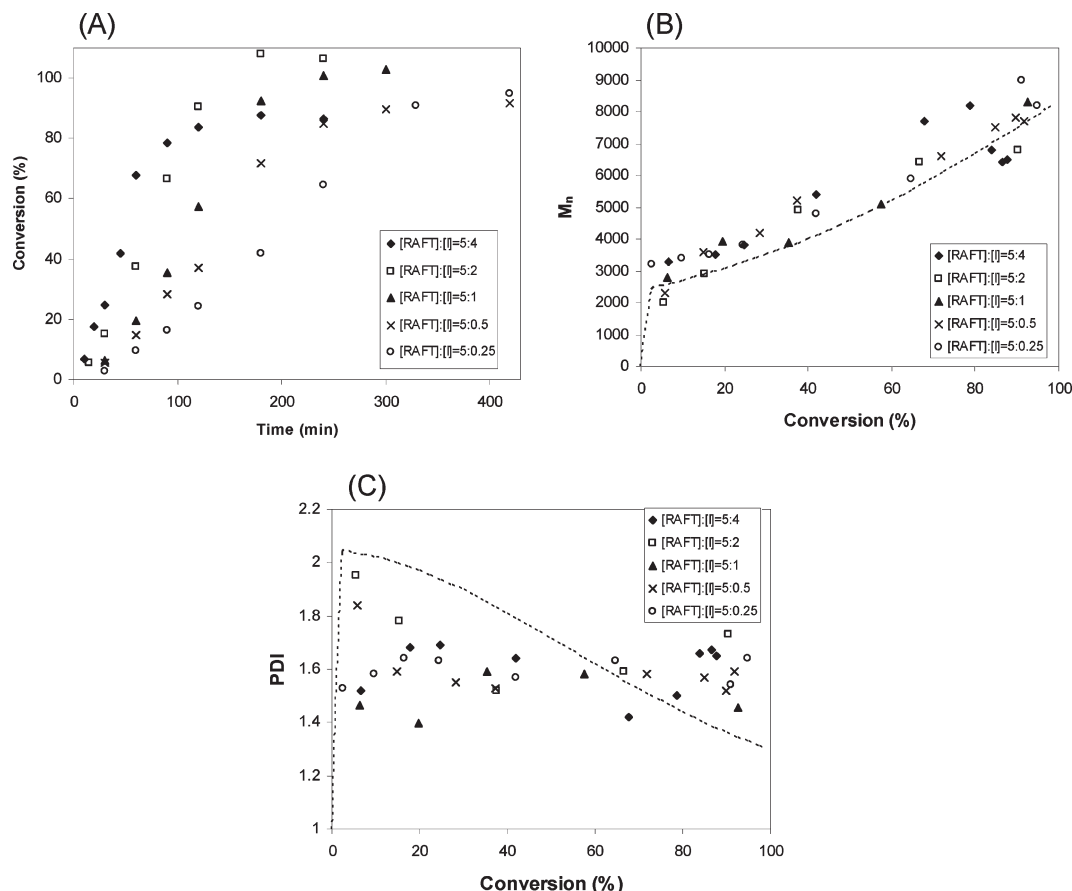


**Figure 7.** Kinetic data for the RAFT-mediated emulsion polymerization of styrene at 70 °C varying initiator concentration in the presence of a constant CTA2 ([1-(*O*-trifluoroethylxanthyl)ethyl]benzene) concentration. (A) conversion vs time, (B) number-average molecular weight ( $M_n$ ) vs conversion, and (C) polydispersity index (PDI) vs conversion. [CTA2] =  $1.56 \times 10^{-2} \text{ mol L}^{-1}$ . Dashed lines are from theory.<sup>49</sup>

the particle size decreases from 38 nm without CTA2 to less than 10 nm (Figure 6D, curve b, [RAFT]:[I] = 1:1). An increase in the [CTA2] above a ratio of 2:1 to initiator results in particles that are so small that they could not be measured by conventional sizing techniques (i.e., dynamic light scattering, DLS). These results are in agreement with simulations in which nucleation of micelles increases with increasing CTA2 concentration (Figure 3C), producing a high particle concentration and very low particle diameter.

A variation in the initiator concentration at a constant CTA2 concentration results in a steady increase in the rate of polymerization (Figure 7A). The  $M_n$  and PDI are similar regardless of initiator concentration (Figure 7B,C), and the particle size for all polymerizations is too low to measure by DLS (see Supporting Information for SEC chromatograms). Again, these results support that exited  $R^\bullet$  radicals play the dominant role in both nucleating micelles and acting as terminators to retard the rate of polymerization. Although a significantly higher amount of initiator is used, the rate is still lower than that found without CTA.

## Conclusion

In summary, we show the successful RAFT-mediated emulsion polymerizations of styrene using two RAFT agents with different chain transfer constants to produce small and stable polystyrene nanoparticles. The MWD of the resulting polymer is well-controlled and could be predicted by theory. With an increase in CTA1 the particle size decreases from 38 to 8 nm, and the particle number concentration  $N_c$  increases from  $2 \times 10^{18}$  to  $2 \times 10^{20}$  particles/L. Although an increase in  $N_c$  should in principle lead to a

faster rate of polymerization, we observe a greater retardation in rate with increasing CTA. The higher the  $C_{tr,RAFT}$ , the greater the initial retardation until consumption of all the RAFT agent. Kinetic simulations solving the Smith–Ewart equations provide mechanistic insight into explain the anomaly between  $R^\bullet$  acting to nucleate micelles and terminate radicals within particles. Small and mobile  $R^\bullet$  radicals form from the fragmentation of RAFT agent, and they can exit particles, re-enter micelles or other particles, re-exit until they either nucleate micelles, or terminate with propagating polymeric chains. This process of exit and re-entry is similar to limit 3 in a conventional emulsion polymerization. The higher micelle nucleation rate through initiation within micelles by  $R^\bullet$  radicals results in smaller and a greater number of particles. Exit is the dominant mechanism for higher nucleation and retardation. And one does not need to invoke either the “slow fragmentation” or “intermediate radical termination” models to explain the effect of CTA concentration on the retardation of rate.

**Acknowledgment.** M.J.M. acknowledges financial support from the ARC Discovery grant and receipt of an Australian Research Council Future Fellowship. We also thank A/Prof. Per Zetterlund for useful comments.

**Supporting Information Available:** SEC traces for the RAFT-mediated emulsion polymerizations are given. This material is available free of charge via the Internet at <http://pubs.acs.org>.

## References and Notes

- (1) (a) Moad, G.; Chong, Y. K.; Postma, A.; Rizzardo, E.; Thang, S. H. *Polymer* **2005**, *46* (19), 8458–8468. (b) Barner, L.; Barner-Kowollik, C.;

- Davis, T. P.; Stenzel, M. H. *Aust. J. Chem.* **2004**, *57* (1), 19–24. (c) Bernard, J.; Favier, A.; Davis, T. P.; Barner-Kowollik, C.; Stenzel, M. H. *Polymer* **2006**, *47* (4), 1073–1080. (d) Whittaker, M. R.; Monteiro, M. J. *Langmuir* **2006**, *22* (23), 9746–9752. (e) Mayadunne, R. T. A.; Jeffery, J.; Moad, G.; Rizzardo, E. *Macromolecules* **2003**, *36* (5), 1505–1513. (f) Wang, W.-p.; You, Y.-z.; Hong, C.-Y.; Xu, J.; Pan, C.-Y. *Polymer* **2005**, *46* (22), 9489–9494. (g) Monteiro, M. J.; Bussels, R.; Beuermann, S.; Buback, M. *Aust. J. Chem.* **2002**, *55*, 433–437.
- (2) (a) Matyjaszewski, K. *Mol. Cryst. Liq. Cryst.* **2004**, *415*, 23–34. (b) Matyjaszewski, K. *Curr. Org. Chem.* **2002**, *6* (2), 67–82. (c) Whittaker, M. R.; Urbani, C. N.; Monteiro, M. J. *J. Am. Chem. Soc.* **2006**, *128* (35), 11360–11361. (d) Huang, J.; Jia, S.; Siegwart, D. J.; Kowalewski, T.; Matyjaszewski, K. *Macromol. Chem. Phys.* **2006**, *207* (9), 801–811. (e) Li, M.; Jahed, N. M.; Min, K.; Matyjaszewski, K. *Macromolecules* **2004**, *37* (7), 2434–2441. (f) An, S. G.; Li, G. H.; Cho, C. G. *Polymer* **2006**, *47* (11), 4154–4162.
- (3) (a) Hawker, C. J.; Bosman, A. W.; Harth, E. *Chem. Rev.* **2001**, *101* (12), 3661–3688. (b) Studer, A.; Schulte, T. *Chem. Rec.* **2005**, *5* (1), 27–35. (c) Hill, N. L.; Braslau, R. Abstracts of Papers, 232nd ACS National Meeting, San Francisco, CA, Sept 10–14, **2006**; POLY-040. (d) Chauvin, F.; Dufils, P.-E.; Gignes, D.; Guillauneuf, Y.; Marque, S. R. A.; Tordo, P.; Bertin, D. *Macromolecules* **2006**, *39* (16), 5238–5250. (e) Lagrille, O.; Cameron, N. R.; Lovell, P. A.; Blanchard, R.; Goeta, A. E.; Koch, R. *J. Polym. Sci., Part A: Polym. Chem.* **2006**, *44* (6), 1926–1940.
- (4) (a) Percec, V.; Guliashvili, T.; Ladislav, J. S.; Wistrand, A.; Stjern Dahl, A.; Sienkowska, M. J.; Monteiro, M. J.; Sahoo, S. *J. Am. Chem. Soc.* **2006**, *128* (43), 14156–14165. (b) Percec, V.; Popov, A. V.; Ramirez-Castillo, E.; Monteiro, M.; Barboiu, B.; Weichold, O.; Asandei, A. D.; Mitchell, C. M. *J. Am. Chem. Soc.* **2002**, *124* (18), 4940–4941. (c) Percec, V.; Popov, A. V.; Ramirez-Castillo, E.; Hinojosa-Falcon, L. A. *J. Polym. Sci., Part A: Polym. Chem.* **2005**, *43* (11), 2276–2280. (d) Percec, V.; Ramirez-Castillo, E.; Hinojosa-Falcon, L. A.; Popov, A. V. *J. Polym. Sci., Part A: Polym. Chem.* **2005**, *43* (10), 2185–2187. (e) Percec, V.; Ramirez-Castillo, E.; Popov, A. V.; Hinojosa-Falcon, L. A.; Guliashvili, T. *J. Polym. Sci., Part A: Polym. Chem.* **2005**, *43* (10), 2178–2184.
- (5) Monteiro, M.; Guliashvili, T.; Percec, V. *J. Polym. Sci., Part A: Polym. Chem.* **2007**, *45*, 1835–1847.
- (6) Gilbert, R. G. *Emulsion Polymerization: A Mechanistic Approach*; Academic Press: London, 1995.
- (7) (a) Fitch, R. M. *Polymer Colloids*; Academic Press: New York, 1997. (b) Lovell, P. A.; E.-A., M. S. *Emulsion Polymerization and Emulsion Polymers*; John Wiley & Sons Ltd.: Chichester, England, 1997.
- (8) Monteiro, M. J.; Hodgson, M.; De Brouwer, H. *J. Polym. Sci., Part A: Polym. Chem.* **2000**, *38* (21), 3864–3874.
- (9) (a) McLeary, J. B.; Klumperman, B. *Soft Matter* **2006**, *2* (1), 45–53. (b) Urbani, C. N.; Monteiro, M. J. RAFT-mediated polymerization in heterogeneous systems. In *Handbook of RAFT Polymerization*; Barner-Kowollik, C., Ed.; Wiley-VCH Verlag GmbH & Co. KGaA: Berlin, 2008; pp 285–314. (c) Monteiro, M. J.; Charleux, B. Living radical polymerisation in emulsion and miniemulsion. In *Chemistry and Technology of Emulsion Polymerisation*; Herk, A. v., Ed.; Blackwell Publishing Ltd.: New York, 2005; pp 111–139. (d) Zetterlund, P. B.; Kagawa, Y.; Okubo, M. *Chem. Rev.* **2008**, *108*, 3747–3794. (e) Cunningham, M. F. *Prog. Polym. Sci.* **2008**, *33*, 365–398.
- (10) Prescott, S. W.; Ballard, M. J.; Rizzardo, E.; Gilbert, R. G. *Macromolecules* **2002**, *35* (14), 5417–5425.
- (11) Prescott, S. W.; Ballard, M. J.; Rizzardo, E.; Gilbert, R. G. *Macromolecules* **2005**, *38* (11), 4901–4912.
- (12) (a) Ferguson, C. J.; Hughes, R. J.; Nguyen, D.; Pham, B. T. T.; Gilbert, R. G.; Serelis, A. K.; Such, C. H.; Hawke, B. S. *Macromolecules* **2005**, *38* (6), 2191–2204. (b) Ferguson, C. J.; Hughes, R. J.; Pham, B. T. T.; Hawke, B. S.; Gilbert, R. G.; Serelis, A. K.; Such, C. H. *Macromolecules* **2002**, *35* (25), 9243–9245.
- (13) (a) Rieger, J.; Osterwinter, G.; Bui, C.; Stoffelbach, F.; Charleux, B. *Macromolecules* **2009**, *42*, 5518–5525. (b) Rieger, J.; Stoffelbach, F.; Bui, C.; Alaimo, D.; Jerome, C.; Charleux, B. *Macromolecules* **2008**, *41* (12), 4065–4068. (c) Rieger, J.; Stoffelbach, F.; Bui, C.; Alaimo, D.; Jerome, C.; Charleux, B. *Macromolecules* **2008**, *41*, 4065–4068.
- (14) (a) de Brouwer, H.; Tsavalas, J. G.; Schork, F. J.; Monteiro, M. J. *Macromolecules* **2000**, *33* (25), 9239–9246. (b) Lansalot, M.; Davis, T. P.; Heuts, J. P. A. *Macromolecules* **2002**, *35* (20), 7582–7591. (c) Tsavalas, J. G.; Schork, F. J.; de Brouwer, H.; Monteiro, M. J. *Macromolecules* **2001**, *34* (12), 3938–3946.
- (15) (a) Urbani, C. N.; Monteiro, M. J. *Macromolecules* **2009**, *42* (12), 3884–3886. (b) Urbani, C. N.; Monteiro, M. J. *Aust. J. Chem.* **2009**, *62* (11), 1528–1532.
- (16) Dunn, A. S. Polymerization in Micelles and Microemulsions. In *Comprehensive Polymer Science*; Allen, G., Bevington, J. C., Eds.; 1989; Vol. 4, pp 219–224.
- (17) (a) Liu, S.; Hermanson, K. D.; Kaler, E. W. *Macromolecules* **2006**, *39* (13), 4345–4350. (b) Hermanson, K. D.; Kaler, E. W. *Macromolecules* **2003**, *36* (6), 1836–1842. (c) Hermanson, K. D.; Liu, S.; Kaler, E. W. *J. Polym. Sci., Part A: Polym. Chem.* **2006**, *44* (20), 6055–6070. (d) Pascual, S.; Monteiro, M. J. *Eur. Polym. J.* **2009**, *45* (9), 2513–2519. (e) Pascual, S.; Urbani, C. N.; Monteiro, M. J. *Macromol. React. Eng.* **2010**, *4* (3), 257–263.
- (18) O'Donnell, J.; Kaler, E. W. *Macromolecules* **2008**, *41*, 6094–6099.
- (19) Sogabe, A.; McCormick, C. L. *Macromolecules* **2009**, *42*, 5043–5052.
- (20) He, G.; Pan, Q.; Remple, G. L. *Macromol. Rapid Commun.* **2003**, *24*, 585–588.
- (21) He, G.; Pan, Q. *Macromol. Rapid Commun.* **2004**, *25*, 1545–1548.
- (22) Adamy, M.; van Herk, A. M.; Destarac, M.; Monteiro, M. J. *Macromolecules* **2003**, *36* (7), 2293–2301.
- (23) Monteiro, M. J.; de Barbeyrac, J. *Macromolecules* **2001**, *34* (13), 4416–4423.
- (24) Monteiro, M. J.; Sjoberg, M.; Van der Vlist, J.; Gottgens, C. M. *J. Polym. Sci., Part A: Polym. Chem.* **2000**, *38* (23), 4206–4217.
- (25) Monteiro, M. J.; Adamy, M. M.; Leeuwen, B. J.; van Herk, A. M.; Destarac, M. *Macromolecules* **2005**, *38* (5), 1538–1541.
- (26) (a) Chern, C.-S.; Wu, L.-J. *J. Polym. Sci., Part A: Polym. Chem.* **2001**, *39*, 898–912. (b) Gerbacia, W.; Rosano, H. L. *J. Colloid Interface Sci.* **1973**, *44* (2), 242–248.
- (27) Monteiro, M. J. *J. Polym. Sci., Part A: Polym. Chem.* **2005**, *43* (15), 3189–3204.
- (28) (a) Charlot, D.; Corpart, P.; Michelet, D.; Zard, S. Z.; Biadatti, T. WO 9858974, 1998. (b) Bell, C. A.; Smith, S. V.; Whittaker, M. R.; Whittaker, A. K.; Gahan, L. R.; Monteiro, M. J. *Adv. Mater.* **2006**, *18*, 582–586.
- (29) Destarac, M.; Charlot, D.; Zard, S.; Franck, X. WO 0075207, 2000.
- (30) Smith, W. V.; Ewart, R. H. *J. Chem. Phys.* **1948**, *16*, 592–599.
- (31) Batt-Coutrot, D.; Robin, J.-J.; Bzducha, W.; Destarac, M. *Macromol. Chem. Phys.* **2005**, *206*, 1709–1717.
- (32) (a) Monteiro, M. J. *J. Polym. Sci., Part A: Polym. Chem.* **2005**, *43* (22), 5643–5651. (b) Johnston-Hall, G.; Monteiro, M. J. *Macromolecules* **2007**, *40* (20), 7171–7179.
- (33) Johnston-Hall, G.; Monteiro, M. J. *J. Polym. Sci., Part A: Polym. Chem.* **2008**, *46*, 3155–3173.
- (34) Full, A. P.; Kaler, E. W.; Arellano, J.; Puig, J. E. *Macromolecules* **1996**, *29*, 2764–2775.
- (35) Maxwell, I. A.; Morrison, B. R.; Napper, D. H.; Gilbert, R. G. *Macromolecules* **1991**, *24*, 1629–1640.
- (36) Maeder, S.; Gilbert, R. G. *Macromolecules* **1998**, *31* (14), 4410–4418.
- (37) de Vries, R.; Co, C. C.; Kaler, E. W. *Macromolecules* **2001**, *34*, 3233–3244.
- (38) Smulders, W.; Gilbert, R. G.; Monteiro, M. J. *Macromolecules* **2003**, *36* (12), 4309–4318.
- (39) Smulders, W.; Monteiro, M. J. *Macromolecules* **2004**, *37*, 4474–4483.
- (40) Ugelstad, J.; Hanson, F. K. *Rubber Chem. Technol.* **1976**, *49*, 536–546.
- (41) Morton, M.; Kaizerman, S.; Altier, M. W. *J. Colloid Sci.* **1954**, *9*, 300–312.
- (42) Butte, A.; Storti, G.; Morbidelli, M. *DEHEMA Monogr.* **1998**, *134*, 497–507.
- (43) Zetterlund, P. B.; Okubo, M. *Macromolecules* **2006**, *39*, 8959–8967.
- (44) Luo, Y.; Wang, R.; Yang, L.; Yu, B.; Li, B.; Zhu, S. *Macromolecules* **2006**, *39*, 1328–1337.
- (45) Manders, B. G.; Chambard, G.; Kingma, W. J.; Klumperman, B.; van Herk, A. M.; German, A. L. *J. Polym. Sci., Part A: Polym. Chem.* **1996**, *34*, 2473–2479.
- (46) Behrman, E. J.; Edwards, J. O. *Rev. Inorg. Chem.* **1980**, *2*, 179–182.
- (47) Griffiths, M. C.; Straunch, J.; Monteiro, M. J.; Gilbert, R. G. *Macromolecules* **1998**, *31* (22), 7835–7844.
- (48) Mueller, A. H. E.; Zhuang, R.; Yan, D.; Litvinenko, G. *Macromolecules* **1995**, *28* (12), 4326–33.
- (49) (a) Guo, J. S.; El-Aasser, M. S.; Vanderhoff, J. M. *J. Polym. Sci., Polym. Chem. Ed.* **1989**, *27*, 691–710. (b) Puig, J. E.; Perez-Luna, V. H.; Perez-Gonzales, M.; Macias, E. R.; Rodriguez, B. E.; Kaler, E. W. *Colloid Polym. Sci.* **1993**, *271*, 114–123.
- (50) Peklak, A. D.; Butte, A. J. *J. Polym. Sci., Part A: Polym. Chem.* **2006**, *44* (20), 6114–6135.

- (51) Barner-Kowollik, C.; Quinn, J. F.; Morsely, D. R.; Davis, T. P. *J. Polym. Sci., Part A: Polym. Chem.* **2001**, *39*, 1353–1357.
- (52) Monteiro, M. J.; de Brouwer, H. *Macromolecules* **2001**, *34*, 349–352.
- (53) Barner-Kowollik, C.; Buback, M.; Charleux, B.; Coote, M. L.; Drache, M.; Fukuda, T.; Goto, A.; Klumperman, B.; Lowe, A. B.; Mcleary, J. B.; Moad, G.; Monteiro, M. J.; Sanderson, R. D.; Tonge, M. P.; Vana, P. *J. Polym. Sci., Part A: Polym. Chem.* **2006**, *44* (20), 5809–5831.
- (54) Monteiro, M. J. *Macromolecules* **2010**, *43* (3), 1159–1168.